BRAIN
ORIGINAL ARTICLE

Serum GFAP levels correlate with astrocyte reactivity, post-mortem brain atrophy and neurofibrillary tangles

Pascual Sánchez-Juan,[1,2] Elizabeth Valeriano-Lorenzo,[1] Alicia Ruiz-González,[1] Ana Belén Pastor,[1] Hector Rodrigo Lara,[3] Francisco López-González,[1] María Ascensión Zea-Sevilla,[1] Meritxell Valentí,[1] Belen Frades,[1] Paloma Ruiz,[1] Laura Saiz,[1] Iván Burgueño-García,[1] Miguel Calero,[1,2,4] Teodoro del Ser[1] and Alberto Rábano[1,2]

See Limberger *et al.* (https://doi.org/10.1093/brain/awae104) for a scientific commentary on this article.

Glial fibrillary acidic protein (GFAP), a proxy of astrocyte reactivity, has been proposed as biomarker of Alzheimer's disease. However, there is limited information about the correlation between blood biomarkers and post-mortem neuropathology.

In a single-centre prospective clinicopathological cohort of 139 dementia patients, for which the time-frame between GFAP level determination and neuropathological assessment was exceptionally short (on average 139 days), we analysed this biomarker, measured at three time points, in relation to proxies of disease progression such as cognitive decline and brain weight. Most importantly, we investigated the use of blood GFAP to detect the neuropathological hallmarks of Alzheimer's disease, while accounting for potential influences of the most frequent brain co-pathologies. The main findings demonstrated an association between serum GFAP level and post-mortem tau pathology ($\beta = 12.85$; $P < 0.001$) that was independent of amyloid deposits ($\beta = 13.23$; $P = 0.02$). A mediation analysis provided additional support for the role of astrocytic activation as a link between amyloid and tau pathology in Alzheimer's disease. Furthermore, a negative correlation was observed between pre-mortem serum GFAP and brain weight at post-mortem ($r = -0.35$; $P < 0.001$). This finding, together with evidence of a negative correlation with cognitive assessments ($r = -0.27$; $P = 0.005$), supports the role of GFAP as a biomarker for disease monitoring, even in the late phases of Alzheimer's disease. Moreover, the diagnostic performance of GFAP in advanced dementia patients was explored, and its discriminative power (area under the receiver operator characteristic curve at baseline = 0.91) in differentiating neuropathologically-confirmed Alzheimer's disease dementias from non-Alzheimer's disease dementias was determined, despite the challenging scenario of advanced age and frequent co-pathologies in these patients. Independently of Alzheimer's disease, serum GFAP levels were shown to be associated with two other pathologies targeting the temporal lobes—hippocampal sclerosis ($\beta = 3.64$; $P = 0.03$) and argyrophilic grain disease ($\beta = -6.11$; $P = 0.02$).

Finally, serum GFAP levels were revealed to be correlated with astrocyte reactivity, using the brain GFAP-immunostained area as a proxy ($\rho = 0.21$; $P = 0.02$).

Our results contribute to increasing evidence suggesting a role for blood GFAP as an Alzheimer's disease biomarker, and the findings offer mechanistic insights into the relationship between blood GFAP and Alzheimer's disease neuropathology, highlighting its ties with tau burden. Moreover, the data highlighting an independent association between serum GFAP levels and other neuropathological lesions provide information for clinicians to consider when interpreting test results.

Received July 10, 2023. Revised December 28, 2023. Accepted January 21, 2024. Advance access publication April 18, 2024

The longitudinal design and correlation with post-mortem data reinforce the robustness of our findings. However, studies correlating blood biomarkers and neuropathological assessments are still scant, and further research is needed to replicate and validate these results in diverse populations.

1 Alzheimer's Centre Reina Sofia-CIEN Foundation-ISCIII, Research Platforms, 28031 Madrid, Spain
2 CIBERNED, Network Center for Biomedical Research in Neurodegenerative Diseases, 28029 Madrid, Spain
3 Banco de Cerebros de la Región de Murcia, Neuropathology Department, 30120 Murcia, Spain
4 Chronic Disease Programme, Instituto de Salud Carlos III, Madrid, Spain

Correspondence to: Pascual Sánchez Juan
Alzheimer's Centre Reina Sofia, Research Platform, C/Valderrebollo 5, 28031 Madrid, Spain
E-mail: psanchezjuan@fundacioncien.es

Keywords: astrocyte; Alzheimer's disease; blood biomarkers; neuropathology; tau

Introduction

In recent years, Alzheimer's disease (AD) diagnostic research has seen remarkable advances. The emergence of several techniques that allow sensitive determination in blood samples of biomarkers of neurodegenerative diseases is one of the most promising. Compared to the traditional immunoassays, these methods are much more accurate in orders of magnitude, and compared to CSF analysis and PET, they hold the potential for more scalable and efficient clinical diagnosis.[1]

Concentrations in the blood of amyloid (amyloid-β_{40} and amyloid-β_{42}) and different phosphorylated tau species (like pTau181, pTau217 and pTau231) correlate with CSF levels of these proteins and with amyloid-PET and tau-PET scans. Neurodegeneration biomarkers such as the neurofilament light chain are also determined in the blood, providing information on disease progression.[2]

More recently, the glial fibrillary acidic protein (GFAP), a proxy of astrocyte reactivity, is correlated with AD physiopathological biomarkers, using CSF or PET analysis as 'gold standards'. Previous publications have shown that GFAP levels in CSF increase rather non-specifically in several neurodegenerative diseases such as AD[3] as well as Creutzfeldt-Jakob disease,[4] Lewy body dementia (LBD) or frontotemporal dementia and amyotrophic lateral sclerosis.[5,6] The determination of GFAP in blood has proven to be a more specific biomarker for AD than in CSF, possibly due to differences in sample stability.[7,8,9]

Several reports using data from research cohorts have correlated blood GFAP levels with cross-sectional tau and amyloid measured by CSF analysis or PET. These studies show that the blood levels of GFAP are associated with amyloid-PET positivity,[10] even in cognitively normal subjects at risk of AD.[11,12] Pereira and colleagues[13] found that GFAP correlated with tau-PET in addition to amyloid-PET. However, correlations between tau-PET and plasma GFAP were no longer significant after controlling for amyloid-PET, and therefore, they concluded that plasma GFAP was mainly related to brain amyloid pathology.

Some studies have suggested that GFAP could be a marker of disease severity: it has been associated with cognition worsening,[3,7,10,14,15] decreased cortical thickness,[8] middle temporal lobe atrophy[10] and higher lateral and third ventricular volumes.[15] GFAP has also been shown to predict conversion from mild cognitive impairment (MCI) to dementia.[14-16] A recent meta-analysis, including studies assessing blood GFAP in eight AD cohorts, showed no significant differences between AD patients and cognitively unimpaired individuals. In addition, they found evidence of publication bias. However, this analysis did not include the new ultrasensitive assays.[17]

Despite significant advances, astrocyte biomarkers in AD remain in their infancy, and some critical uncertainties and issues must be addressed before they can be used in clinical practice. A fundamental step is clarifying the association between blood GFAP levels and post-mortem neuropathology. Only a dozen studies correlate blood biomarkers with post-mortem neuropathology,[17-30] and as far as we know, only three provide data on GFAP.[18-20] The neuropathological validation of AD biomarkers is a fundamental step towards their clinical implementation. Even for the best-established, like some of the phosphorylated tau species, uncertainties still exist. For instance, recent evidence based on PET correlations suggests that some of these biomarkers may be more related to amyloid than to tau load.[21]

The increasingly complex patterns of neuropathological lesions of the ageing brain could be one crucial factor explaining biomarker behaviour, which has not been fully considered. The reported associations between GFAP levels, especially in CSF, and different combinations of neurodegenerative pathologies need further clarification. As far as we know, only one previous article[19] has correlated pre-mortem GFAP levels with post-mortem Lewy body and TDP-43 pathologies. However, the relation with other co-pathologies like ageing-related tau astrogliopathy (ARTAG), which directly targets astrocytes, has not been studied. It is, therefore, unclear how several neurodegenerative diseases in the brain influence the performance of the biomarkers.

Finally, there are few data on individuals in the late stages of the disease. Most studies have correlated GFAP with core AD biomarkers (amyloid-β and tau species) determined by PET or CSF analysis at early or middle stages in highly selected individuals from research cohorts. In contrast, there is scant 'real-world' information on elderly individuals with advanced dementia.

CIEN Foundation is a research institute located within the facilities of a large nursing home dedicated to dementia patient care. Our unique setting allows us to carry out the Vallecas Alzheimer Center Study (VACS). This prospective cohort follows residents entering a brain donation program from admission to the centre, with repeated neuropsychological assessments, brain MRI and biological sample collections. This design facilitates minimal time between pre-mortem blood sampling and brain collection, allowing precise

correlations between biomarker levels and brain pathology. Using the ultrasensitive single molecule array (Simoa), we quantified serum GFAP in the pre-mortem samples of the VACS cohort and from two previous assessments, at admission to the nursing home and at an intermediate time point.

Our main goal was to better understand the relationship between serum GFAP levels and their time trajectory with disease progression and the neuropathological findings observed in moderate-severe dementia patients. In a clinicopathological cohort in which GFAP level determination was exceptionally close to the neuropathological assessment, we analysed the relationship of this biomarker with proxies of disease progression such as cognitive decline or brain weight. Most importantly, we aimed to validate the role of blood GFAP in detecting the neuropathological hallmarks of AD and to account for potential influences of the most frequent brain co-pathologies.

Materials and methods

Study participants and design

The characteristics of the patients and cohort have been described elsewhere.[22] In brief, this study was based on post-mortem brain donations from the VACS cohort. Routine clinical evaluation of patients in the VACS cohort includes baseline and biannual assessment of several cognitive, functional and behavioural traits.[22] We recorded details including sex, age at disease onset according to medical records and caretaker interviews, global deterioration stage and severe Mini-Mental State Examination (sMMSE)[23] paired with GFAP determination in serum at three time points: (i) at the admission to the nursing home (T1); (ii) at an intermediate time point (T2); and (iii) the at post-mortem evaluation (T3). We included all individuals whose brains had already been collected and provided pre-mortem blood samples for our analyses.

Serum GFAP determination

All participants from the VACS were required to fast for at least 2 h before the medical assessment. Venous blood was drawn and collected into serum separator tubes (SST™ II advance, BD Vacutainer®). Within 2 h of collection, samples were centrifuged (10 min at 1700*g* at 4°C) and stored at −80°C. Serum GFAP concentration was measured using the ultrasensitive Simoa on the Quanterix SR-X platform (Quanterix). We analysed, when available, three serum sample points from everyone (T1, T2 and T3). All samples from the same individual were analysed in the same plaque.

Neuropathological workup

Main neuropathological procedures for brain extraction and immediate processing have been described previously.[24] Shortly after extraction, the brain was weighed and bisected through a mid-sagittal section. The right half hemibrain was fast-frozen, while the left hemibrain was fixed by immersion in 4% buffered formaldehyde for complete neuropathological processing. After 3 weeks of fixation, the left cerebral hemisphere was cut in serial coronal slices, the cerebellum in parasagittal slices and the brainstem in transversal slices. Multiple tissue blocks were dissected from cortical and subcortical regions for paraffin embedding, and 4 µm paraffin sections were obtained for routine haematoxylin/eosin (H/E) examination and immunohistochemistry. All histological assessments of this study were performed under a Nikon Eclipse 90i optical microscope using white light and apochromatic optics.

Neuropathological classification of cases was performed according to published consensus criteria. For that purpose, a panel of immunohistochemical stains was applied to selected brain regions based on the following primary antibodies: amyloid-β protein (Dako, code: M087201-2), tau AT100 (ThermoFisher Invitrogen, code: MN1060), ubiquitin (Abcam, code: ab7254), α-synuclein (Leica Biosystems, code: 1 ml NCL-L-ASYN), and TDP-43 (Proteintech®, code: 10782-2-AP), according to the manufacturer's instructions. For GFAP immunostaining, a rabbit polyclonal antibody was used (Code-Nr Z 0334, Dakocytomation) that specifically depicts astrocytes in brain tissue. Microglia was identified with mouse anti-Human CD68 monoclonal antibody, clone PG-M1 (Code-Nr M 0876, Dakocytomation). In brain tissue, CD68 is present both in microglia and in blood-derived macrophages. Immunohistochemistry was performed on a Dako Link 48 Autostainer.

For the assessment of Alzheimer's disease neuropathological change (ADNC) (either null, low, intermediate or high probability), we employed the ABC method recommended by the National Institute on Aging (NIA), including the evaluation of Thal amyloid stage (0–5), NIA-A stage (0–3), Braak tau stage (0–VI), NIA-B stage (0–3) and Consortium to Establish a Registry for Alzheimer's Disease (CERAD) NIA-C stage (0–3).[25] Lewy body pathology was assessed through Braak α-synuclein staging (0–6)[26] and Lewy body Pathology Consensus (LPC) classification (0–5).[27] For the assessment of cerebrovascular disease associated with dementia, we used the total vascular score (TVS) defined by Deramecourt *et al*.[28] (0–20) that includes partial assessment of vascular pathology in the frontal and temporal lobes (0–6), basal ganglia (0–4) and hippocampus (0–4). Vascular cognitive impairment neuropathology guidelines (VCING) criteria for assessing vascular pathology burden in dementia patients was also applied.[29] Additionally, TDP-43 proteinopathy was evaluated according to the definition and staging of limbic-predominant age-related TDP-43 encephalopathy (LATE) (0–3).[30] The stage of hippocampal sclerosis (HS) (0–4), as defined recently by our group,[24] was also assessed in all patients. HS staging was performed at two coronal levels of the hippocampus, separated by the tip of the uncus: head (anterior HS) and body (posterior HS). Other frequently combined pathologies assessed were argyrophilic grain disease (AGD) (Saito stages, 0–3)[31] and ARTAG.[32] The latter was registered as present or absent, both in the medial temporal lobe and the cerebral neocortex/yuxtacortical white matter.

For the quantitative analysis of GFAP immunostaining, five randomly assigned regions were imaged per section in the superior entorhinal cortex (layers I–III) and basolateral amygdala, using a Nikon Eclipse 90i T1 microscope. Image analysis and quantification were performed using the open-source software CellProfiler.[33] A CellProfiler pipeline was designed to quantify the number of immunostained pixels, allowing the calculation of the areas. For CD68 quantification, a similar pipeline was designed, but we only evaluated the superior entorhinal cortex (layers I–III).

Statistical analyses

Data analyses and visualization were performed using R version 4.2.1. Differences in demographics and clinical characteristics across the groups were assessed with the chi-square statistic for categorical variables or Student's *t*-tests for continuous variables. Two subjects whose GFAP levels were 4 standard deviations (SD) above the mean were removed from the analysis. The distribution of GFAP levels in serum was skewed, so the values were normalized by the BoxCox transformation function (tfGFAP), supported by the fpp package. After the statistical analysis was performed, and in

the cases when the information on the original values was required for descriptive purposes, the following formula was used to convert the tfGFAP value to its raw value: $\text{rawGFAP} = (\text{tfGFAP} \times lambda_{T(i)} + 1)^{(1/lambda_{T(i)})}$ where $T(i)$ is the respective time point.

Pearson's and Spearman's correlations were used to assess the strength of the association of serum GFAP with relevant covariates and cognition.

The diagnostic accuracy of serum GFAP was assessed using receiver-operating characteristic (ROC) curves, with sex, estimated age at onset and age at serum extraction as covariates. We employed the AROC package to analyse ROC curves adjusted by covariates. The DeLong test was conducted to compare two correlated ROC curves analysing the differences in their respective areas under the curve (AUC) using the pROC package.

Linear mixed-effect models (LMMs) were performed to investigate the rate of change of serum GFAP and the longitudinal change of cognition (sMMSE) over time. The LMM were independent analyses and included a random intercept per participant, and a random slope of GFAP or sMMSE, capturing interindividual variability. For these analyses, we considered only subjects with two or three available data-points in both measures, serum GFAP and sMMSE, and subjects with only one determination were removed.

Three independent models (an unconditional LMM, the interaction between time and ADNC, and a conditional LMM) were performed with serum GFAP as the dependent variable and age at serum extraction as the time variable. ADNC was an independent variable in the conditional LMM and adjusted by sex, age at onset and number of days between blood extraction date and death. Covariates were centralized prior to analyses. To investigate the relationship between the rate of change of GFAP and cognition rate, we extracted the coefficients of both conditional LMM. Next, a multiple regression was performed with cognition rate as the dependent variable, GFAP growth as the independent variable and adjustment for age at onset, number of days between extraction date and death date, and sex.

Multiple regression analyses were performed to test the association between serum GFAP at the pre-mortem evaluation (T3) and post-mortem pathological measures of brain atrophy, the ADNC score (based on measures of NIA-A, NIA-B and NIA-C) and the presence of other brain co-pathologies that were dichotomized following the approach reported by Nichols *et al.*[34] All models were adjusted by relevant covariates (age at extraction, age at onset, number of days elapsed between extraction and death and sex).

Structural Equation Modelling (SEM) using the lavaan package was performed to test the hypothesized conceptual model based on path analysis. SEM is a multivariate technique combining factor analysis and multiple regression. The weighted least squares means and variance adjusted estimation were used to analyse ordinal outcomes.[35] To assess how well the specified model reproduced the observed the covariance matrix, four (two absolute and two incremental) fit indices were employed: standardized root mean residual (SRMR), root mean square error of approximation (RMSEA), comparative fit index (CFI) and the Tucker–Lewis index (TLI).[36] A path analysis was specified based on the hypothesized conceptual model by assigning direct and indirect (mediating) effects of NIA-A and NIA-C on the dependent variable NIA-B, with serum GFAP in the mediator role. The effects were adjusted by age at extraction at T3 and sex.

Finally, we used Spearman partial correlation coefficients to correlate between GFAP and CD68-immunostained areas in brain regions and serum GFAP levels.

Ethical approval

Local health authorities have approved the VACS patient follow-up program at the Queen Sofía Alzheimer's Center (Ref: MCB/RMSFC, Expte: 12672). All brain donations were carried out under informed consent provided by a relative or proxy, as approved by the research ethics board of the Carlos III Research Institute. All tissues and blood samples used in the study were transferred by the local biobank (CIEN Tissue Bank) according to approved protocols. The CIEN Tissue Bank is a biobank authorized by local and national health authorities (Registry number 0000741).

Results

Table 1 shows the characteristics of the participants who provided samples at the three selected time points. One hundred and thirty-nine patients were included in the study; 113 (81.3%) were female. Their mean age (SD) at admission to the nursing home was 83.1 (±6.0) years, and their dementia syndrome was predominantly moderate-severe [86% Global Deterioration Scale (GDS) score >4]. Most cases had a pathological diagnosis of AD based on an ADNC score higher than two (94.1% at T1, 93.8% at T2, 92.1% at T3). The main primary pathological diagnosis was AD ($n = 89$, 78.4%); vascular dementia ($n = 11$, 10.1%) and frontotemporal lobar degeneration due to tau deposits ($n = 10$, 8.6%) were the next most highly diagnosed diseases, and there were a few cases with LBD ($n = 3$, 2.2%) or HS ($n = 1$, 0.72%). Remarkably, the average time from pre-mortem serum extraction (T3) to neuropathological assessment was only 139 days.

We did not find a significant correlation between age at serum collection and tfGFAP levels at any of the three time points in the whole dementia sample ($r_{T1} = 0.03$, $P = 0.78$; $r_{T2} = 0.10$, $P = 0.42$; $r_{T3} = 0.14$, $P = 0.11$) or in the subgroup of AD dementia cases ($r_{T1} = 0.07$, $P = 0.53$; $r_{T2} = 0.13$, $P = 0.33$; $r_{T3} = 0.16$, $P = 0.07$). In AD, younger age at disease onset correlated mildly with higher tfGFAP levels at T1 and T2 but not at time point 3 ($r_{T1} = -0.25$, $P = 0.02$; $r_{T2} = -0.29$, $P = 0.03$; $r_{T3} = -0.15$, $P = 0.10$). Age at death did not correlate with tfGFAP levels at any of the three time points ($r_{T1} = -0.07$, $P = 0.48$; $r_{T2} = -0.13$, $P = 0.31$; $r_{T3} = 0.08$, $P = 0.37$). In addition, when we compared tfGFAP levels between males and females, we found significantly higher levels in females in both the AD cases (mean = 37.76 versus 33.39; $P = 0.03$) and the whole sample (mean = 36.95 versus 32.49; $P = 0.02$) but only at T3. Finally, ApoE did not show a significant relationship with the levels of serum GFAP at any time point ($r_{T1} = 0.08$, $P = 0.41$; $r_{T2} = -0.06$, $P = 0.66$; $r_{T3} = 0.05$, $P = 0.54$) in the total sample or in the AD group (r_{T1}=0.01, $P = 0.95$; $r_{T2} = -0.12$, $P = 0.38$; $r_{T3} = -0.03$, $P = 0.71$).

GFAP correlates with cognition in moderate-advanced dementia patients

We performed a cross-sectional analysis correlating tfGFAP serum levels with the sMMSE test in the subgroups of individuals with AD and the whole sample (Supplementary Table 1). In all dementia patients, we found a negative correlation between cognitive performance and tfGFAP levels at T1, T2 and T3 ($\rho_{T1} = -0.22$, $P = 0.05$; $\rho_{T2} = -0.51$, $P < 0.001$; $\rho_{T3} = -0.28$, $P = 0.002$). When analysed separately, AD dementia individuals also showed a significant negative correlation between the sMMSE and tfGFAP levels at T1, T2 and T3 ($\rho_{T1} = -0.19$, $P = 0.11$; $\rho_{T2} = -0.48$, $P < 0.001$; $\rho_{T3} = -0.27$, $P = 0.005$), meaning that the higher the tfGFAP serum level, the lower the cognitive performance during the last two follow-up visits.

Table 1 Descriptives

	Cases at time point 1	Cases at time point 2	Cases at time point 3
n	102	64	139
Age at serum collection, years, mean (SD)	83.5 (5.7)	87.0 (6.0)	87.7 (6.4)
Females %	83.3	87.5	81.3
sMMSE score mean (SD)	5.7 (6.5)	1.8 (4.15)	2.5 (4.8)
GDS (score 5–7), %	86	98	98
APOE e4 carriers, %	44.1	45.3	46.0
GFAP levels (pg/ml), mean (SD)	444.9 (214.2)	539.7 (253.1)	613.2 (340.4)
GFAP levels (pg/ml), median (IQR)	395.7 (323.12–512.35)	491.6 (369.1–650.4)	568.5 (365.52–779.41)
Days from serum collection to death, mean (SD)	2031.0 (1021.5)	1252.9 (190.3)	138.9 (130.9)
ADNC, 0/1/2/3	0/6/13/83	0/4/6/54	1/10/21/107
AD neuropathologically confirmed/non-AD dementia	96/6	60/4	128/11

Data are mean, standard deviation (SD), median, interquartile range (IQR), percentages (%) or frequencies. AD = Alzheimer's disease; ADNC = Alzheimer's disease neuropathologic change; GDS = Global Deterioration Scale; sMMSE = severe Mini-Mental State Examination.

GFAP levels differentiate pathologically defined Alzheimer's disease from other dementias

The levels of tfGFAP were higher in AD dementia cases (defined as ADNC ≥ 2) than in the other dementia diagnosis (Fig. 1), ranging from a 1.9-fold increase at T1, a 1.4-fold increase at T2 and a 2.0-fold increase at T3. They were significantly higher at the first and third time points ($t_{T1} = -2.817$, $P = 0.03$; $t_{T2} = -1.501$, $P = 0.22$; $t_{T3} = -3.254$, $P = 0.01$).

Despite the low numbers of non-AD cases, ROC analysis showed that GFAP had good discriminative power, ranging from an AUC of 0.91 [95% confidence interval (CI): 0.70–0.99] in T1 to 0.83 (95%CI: 0.73–0.90) and 0.79 (95%CI: 0.74–0.88) at T2 and T3, respectively. Sex, age at extraction and age at onset were included as covariates in those analyses. The Delong method showed that there were no significant differences between them ($\Delta AUC_{T1-T2} = 0.73$, $P = 0.47$; $\Delta AUC_{T2-T3} = -0.30$, $P = 0.77$; $\Delta AUC_{T1-T3} = 0.60$, $P = 0.55$).

GFAP longitudinal analysis

We assessed the longitudinal change in GFAP and its association with the presence of AD pathology at death (see Supplementary Table 2 for descriptive information). First, we fitted an unconditional LMM (Table 2) to estimate the rate of change, with age at extraction as the time variable. Next, we tested whether ADNC pathology as a predictor adjusted by relevant covariates would improve the unconditional LMM of tfGFAP levels. The conditional LMM explained 29% of the variability in the longitudinal trajectory of tfGFAP levels, 18% more than the unconditional model. The former model significantly improved the latter [$\Delta\chi^2 = 46.986$, Δdf (degrees of freedom) = 5, $P < 0.001$] and estimated that the tfGFAP levels increased by 1.07 units per 1 SD at the time (centralized at mean = 86.4 years, SD = 6.3 years) after controlling for relevant covariates (Table 2). Based on the conditional LMM, the older age at extraction time, the higher the tfGFAP levels. Furthermore, patients with a high AD pathology at death (ADNC = 3) had significantly more tfGFAP levels at baseline than the reference group (β = 1.63; $P = 0.003$), and individuals with younger age at disease onset had significantly higher tfGFAP levels at baseline than those with later onset (β = –1.10; $P < 0.001$). Next, we tested the interaction term between tfGFAP and the ADNC (Table 2), revealing that the association between the rate of biomarker change and the degree of pathology at death was not statistically significant (Time × Intermediate ADNC: β = 1.04, $P = 0.121$; Time × High ADNC: β = 0.82, $P = 0.093$). Figure 2 shows tfGFAP levels across time estimated by the LMM and stratified by their ADNC at death.

GFAP rate of change and cognitive changes

We assessed whether the rate of change of tfGFAP was associated with the rate of change of sMMSE. After extracting their individual intercepts and slopes estimated for their respective unconditional LMM, a multiple regression was performed with adjustment for age at disease onset, number of days between extraction date and death date, and sex. The results (Supplementary Table 3) show a negative but not significant association between the change rates of both measures (β = –1.25; $P = 0.47$) considering the complete data. No significant association was seen between the tfGFAP rate of change and the initial cognitive performance (β = –9.53; $P = 0.11$). A sensitivity analysis was performed with individuals who were classified with higher ADNC (Supplementary Table 3), and the results were similar to previous findings; no significant association was found between the rate of change in serum GFAP and both the initial score and the rate of change in cognition.

GFAP significantly correlates with brain weight

TfGFAP levels were negatively correlated with brain weight at all sample time points both in the whole sample ($r_{T1} = -0.24$, $P = 0.02$; $r_{T2} = -0.41$, $P = 0.001$; $r_{T3} = -0.39$, $P < 0.001$) and in the subgroup of AD cases ($r_{T1} = -0.24$, $P = 0.02$; $r_{T2} = -0.40$, $P = 0.002$; $r_{T3} = -0.35$, $P < 0.001$) (Fig. 3).

This association was still significant (β = –0.02; $P = 0.008$) at T3 when we adjusted by age at serum extraction, age at disease onset, time from extraction to death, and sex (Supplementary Table 4).

Pre-mortem serum GFAP is associated with Alzheimer's disease neuropathological burden

We found that tfGFAP levels at T3, the closest to the post-mortem assessment, were associated with ADNC stages when adjusted by covariates (Intermediate ADNC: β = 8.48, $P = 0.02$; High ADNC: β = 10.35, $P < 0.015$; Table 3). When we disaggregated ADNC into its components in an independent analysis, we observed that NIA-B (Intermediate NIA-B: β = 7.17, $P = 0.046$; High NIA-B: β = 12.85, $P < 0.001$) and NIA-C (Intermediate NIA-C: β = 0.74, $P = 0.80$; High NIA-C: β = 4.69, $P = 0.036$) were also associated with tfGFAP levels (Table 3). In all cases, the higher the disease stages, the higher the tfGFAP levels.

Similar results were obtained in T1 and T2; NIA-B achieved a significant association with tfGFAP and better goodness-of-fit indexes in both sample points (Supplementary Table 5). When we entered

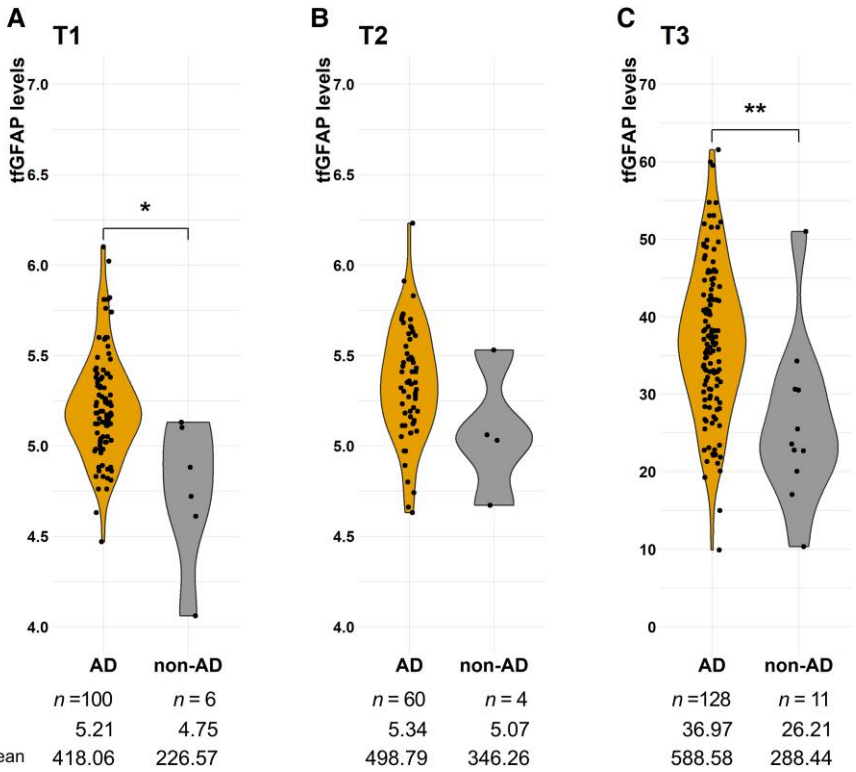

	AD	non-AD	AD	non-AD	AD	non-AD
	n =100	*n* = 6	*n* = 60	*n* = 4	*n* =128	*n* = 11
tfGFAP Mean	5.21	4.75	5.34	5.07	36.97	26.21
[a]raw GFAP Mean	418.06	226.57	498.79	346.26	588.58	288.44

Figure 1 TfGFAP levels by the pathological group at the three sample points.

[a]The mean value of tfGFAP was converted to the raw GFAP value using the BoxCox transformation (see 'Materials and methods' section). *P < 0.05, **P < 0.01. AD = Alzheimer's disease; T1–3 = time points 1–3; tfGFAP = GFAP levels normalized by the BoxCox transformation function.

NIA-A, NIA-B and NIA-C plus covariates in a single model, we found that NIA-B was the only independent variable associated with tfGFAP levels (β = 13.23; *P* = 0.021) (Table 3). Furthermore, the model composed of NIA-B obtained a higher explained variance than other models.

Pre-mortem serum GFAP is associated with HS and argyrophilic grain disease independently of AD

We performed a similar analysis with other neuropathological variables. Lineal models were built with every pathological staging plus covariates at the pre-mortem sample. We found that posterior HS and LATE staging were significantly and positively associated with tfGFAP levels; in contrast with AGD, which was negatively associated with tfGFAP levels.

Next, to assess the effect of each neuropathological factor independently of AD pathology, we repeated the same analysis but included ADNC staging in all the models. We found that tfGFAP levels were associated, independently of AD pathology, with AGD and posterior HS (Supplementary Table 6).

Serum GFAP, as a proxy of astrocyte reactivity, mediates in brain tau load

We fitted two partial mediation models to test the hypotheses of the role of amyloid-dependent astrocytic activation in the development of tau load. We used GFAP levels of the pre-mortem sample as a proxy of astrocytic activation. Figure 4 schematizes both models and shows their main results. The first model accounted for 57% of the variance in NIA-B, while the second model accounted for 49%. Both models achieved acceptable goodness-of-fit indexes, RMSEA = 0.067 and 0.057, CFI = 0.98 and 0.98, TLI = 0.96 and 0.97 and SRMR = 0.052 and 0.057, respectively (*n* = 138).

The direct effects of both models evidenced that individuals with higher NIA-C (β=0.65, *P* < 0.001) and NIA-A (β = 0.58, *P* < 0.001) stages were significantly associated with higher tau load in post-mortem brain tissue.

Model 1 showed that the highest post-mortem NIA-C stage (individuals categorized as NIA-C = 3) was associated with higher amounts of serum GFAP in T3 (β = 0.24, *P* < 0.001), and, in turn, levels of serum GFAP were positively associated with the post-mortem tau load (β = 0.27; *P* < 0.001). Similarly, model 2 showed that the highest post-mortem NIA-A stage (individuals categorized as NIA-A = 3) was associated with higher amounts of serum GFAP in T3 (β = 0.32, *P* < 0.001), and likewise, serum GFAP was positively associated with tau load in post-mortem brain tissue (β = 0.25; *P* = 0.01). Analyses using a 95% CI lent additional support for indirect (mediating) effects in both Model 1 (β = 0.007, *P* = 0.02) and Model 2 (β = 0.008, *P* < 0.001). The proportion of the indirect effect with respect to the total effect was 9% for the first model and 12% for the second (Supplementary Table 7).

Therefore, serum GFAP acted in both models as a mediator between amyloid (NIA-C and NIA-A) and tau (NIA-B), indicating that astrocytic activation plays a role in the interaction between brain amyloid and tau load.

Pre-mortem serum GFAP levels correlate with GFAP and CD68-immunostained brain areas

To elucidate the correlation between serum GFAP levels and astrocyte reactivity, we conducted a quantitative analysis of the

Table 2 Associations between longitudinal changes of levels of serum tfGFAP and the level of post-mortem neuropathology

Model	β (95%CI)	P-value	[a]R^2_M	[b]R^2_C
[c]**Unconditional LMM**				
Intercept	12.25 (11.93, 12.57)	<0.001	0.11	0.65
Slope, time	0.65 (0.33, 0.99)	<0.001		
[d]**Interaction time:neuropathology**				
Intercept	10.57 (9.27, 11.92)	<0.001	0.17	0.64
Slope, time	−0.13 (−1.05, 0.86)	0.78		
Time:Intermediate ADNC	1.04 (−0.30, 2.36)	0.12		
Time:High ADNC	0.82 (−0.16, 1.77)	0.09		
[e]**Conditional LMM to predict the longitudinal trajectory of tfGFAP levels**				
Intercept	10.78 (9.63, 11.85)	<0.001	0.29	0.65
Slope, time	1.07 (0.77, 1.37)	<0.001		
[f]Intermediate ADNC	1.23 (−0.13, 2.62)	0.07		
[f]High ADNC	1.63 (0.53, 2.82)	0.003		
Time extraction T1-exitus, days	0.14 (−0.15, 0.42)	0.33		
Estimated age of onset	−1.10 (−1.47, −0.74)	<0.001		
Sex	0.12 (−0.59, 0.82)	0.74		

Covariates included in the models are age at serum extraction, estimated age at onset, number of days between last serum collection and death date, and sex. ADNC = Alzheimer's disease neuropathological change; LMM = linear mixed-effect model; T1 = time point 1; tfGFAP = GFAP levels normalized by the BoxCox transformation function.

[a]Conditional R^2 estimates the fraction of the variance explained by the fixed effects in the model.

[b]Marginal R^2 estimates the fraction of the variance explained by the fixed and random effects.

[c]Model equation: $tfGFAP_{T3} = \beta_0 + \beta_1 \times Time + (Time \mid ID)$.

[d]Model equation: $tfGFAP_{T3} = \beta_0 + \beta_1 \times Time + \beta_2 \times ADNC + \beta_3 \times Time{:}ADNC + (Time \mid ID)$.

[e]Model equation: $tfGFAP_{T3} = \beta_0 + \beta_1 \times Time + \beta_2 \times ADNC + \beta_3 \times T1\text{-}exitus + \beta_4 \times Age\ onset + \beta_5 \times Sex + (Time \mid ID)$.

[f]The reference group is the Non-AD/Lower neuropathology score at death (ADNC = 0 and 1). Intermediate ADNC corresponds with a neuropathology score of 2 at death (ADNC = 2). High ADNC corresponds with a neuropathology score of 3 at death (ADNC = 3).

immunostained GFAP area, as a surrogate measure, in two distinct brain regions (the entorhinal cortex and the amygdala) across our entire study cohort ($n = 139$). Despite the absence of a significant correlation in the amygdala, a statistically significant positive partial correlation, adjusted for sex and age at sample collection, emerged in the entorhinal cortex ($r = 0.21$; $P = 0.02$). Subsequent stratification of individuals based on their tau Braak stage revealed a heightened and more significant positive correlation in those with elevated tau load (Braak stage > 4) compared with those with lower ($r = 0.21$; $P = 0.04$ versus $r = 0.15$; $P = 0.5$, respectively). When we pooled the data from both brain regions, we found a borderline positive correlation ($r = 0.18$; $P = 0.05$), that again was stronger in the individuals with advanced Braak ($r = 0.22$; $P = 0.02$) (Supplementary Table 8). Also, we found that the GFAP immunostained area in the entorhinal cortex negatively correlated with brain weight in the crude analysis ($r = -0.18$; $P = 0.04$) and was borderline significant when we adjusted by age at collection and sex ($r = -0.17$; $P = 0.06$); however, this association was not present in the amygdala. (Supplementary Table 9).

Additionally, we aimed to investigate the relationship between serum GFAP and microglial activation. In a subsample of advanced AD patients (Braak > 4) ($n = 39$), we used the immunostained CD68 area as a proxy for microglial activation. We observed a negative correlation between the area of CD68 immunoreactivity in the entorhinal cortex and serum GFAP adjusted by age at collection and sex ($r = -0.40$; $P = 0.01$). The immunostained area of CD68 did not correlate with brain weight nor with the immunoreactivity area of GFAP. (Supplementary Table 10).

Discussion

In this study, we investigated longitudinal measures of serum GFAP from institutionalized patients with moderate/severe dementia in conjunction with their post-mortem neuropathological data. Our main findings offer robust evidence about the association between serum GFAP levels and tau pathology, supporting its role as a diagnostic biomarker and offering mechanistic insights about the potential role of astrocyte reactivity as a mediator between amyloid and tau pathology in AD. Additionally, we provide evidence supporting serum GFAP as a biomarker for astrocyte reactivity through a quantitative examination of GFAP immunostaining.

The time interval between the serum extraction and the brain post-mortem study, 139 days on average, is the lowest reported in the literature for neuropathological validation of blood biomarkers of AD, minimizing possible confounding factors and providing high temporal precision. Therefore, based on our results, we can safely conclude that GFAP serum levels are a good proxy of AD neuropathology. Previous reports have demonstrated its cross-sectional association with tau and amyloid CSF or PET measurements in early AD, MCI or even cognitively healthy individuals.[10,11,12] However, our design provides a more comprehensive understanding of the role of GFAP as an AD biomarker, expanding the knowledge of its potential clinical use beyond the limitations of cross-sectional data and potential publication bias.

To our knowledge, only three previous studies have evaluated GFAP blood levels and postmortem AD pathology.[18-20] Winder and colleagues[18] studied AD and vascular neuropathological changes in a community-based cohort ranging from 72 to 84 individuals with a maximum time from blood sample to the autopsy of 2 years. Even though they found a trend of association between GFAP and neuropathological lesions of AD, their results did not reach statistical significance. More recently, Salvadó and colleagues[19] tested several plasma biomarkers, including GFAP, in 105 individuals with an average of 482 days between blood extraction and death. They correlated GFAP plasma levels with semiquantitative assessments of AD pathology and, similar to our results, GFAP was only independently associated with neurofibrillary tangles. In that study, the association with plaque load lost its statistical significance after adjusting by tangle load. Another recent study has also shown that GFAP predicts Braak stage scores.[20]

In addition to validating GFAP determination with neuropathological data, our analysis provides information about its diagnostic performance in patients with advanced dementia, a population rarely tested with biomarkers. Despite the unspecific nature of GFAP, and even in the *a priori* challenging scenario of old age advanced dementia patients with frequent co-pathology, GFAP showed a good discriminative power between neuropathologically confirmed AD dementias versus non-AD dementias. Even though we saw a slight decrease in diagnostic accuracy from T1 to T3, the DeLong test showed no differences between them. Also, our longitudinal analyses offer helpful information from a clinical perspective. The model showed that GFAP levels increased with time in demented individuals. We found that, independently of the final neuropathological diagnosis (AD dementia versus non-AD), other factors influenced GFAP levels. Individuals younger at disease onset had higher serum GFAP levels. In contrast, we found no sex

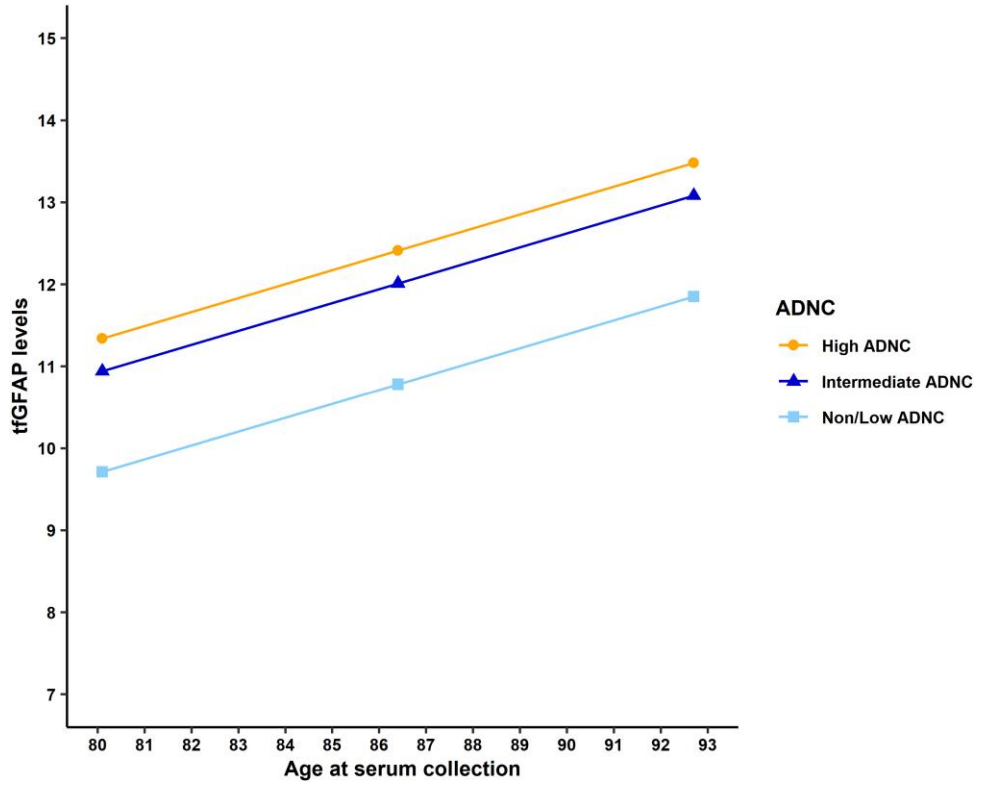

Figure 2 Predicted values of serum tfGFAP by the age of extraction and by the level of post-mortem neuropathology. The age of extraction is centred at 86.4 years (1 SD = 6.3 years). The predicted values were calculated controlling by sex (female), estimated age at onset (mean = 75.11 years, 1SD = 7.5), and the time elapsed between time-point 1 and death date (mean = 2146 days, 1 SD = 992.457). ADNC = Alzheimer's disease neuropathologic change; SD = standard deviation; tfGFAP = GFAP levels normalized by the BoxCox transformation function.

influences; although females tended to have higher GFAP levels, the differences were non-significant when included in the multivariate model.

Our study shows that serum GFAP levels are robustly associated with the disease's severity from a clinical and neuropathological perspective. As has been shown before in less advanced patients, higher GFAP levels correlated with poor cognition,[10] even in cognitively normal subjects at risk of AD.[11,12] An observation of our study, not reported before, is that brain weight at post-mortem was also negatively associated with pre-mortem serum GFAP. In contrast to what has been described for other AD markers, like CSF tau[37] or amyloid levels,[38] in our series GFAP did not seem to plateau and it increased until the pre-mortem exam. This result should be interpreted in light of the polymorphic and evolving role of the astrocyte in AD. It has been reported that during the late stages of the disease, astrocytes may undergo a state of atrophy and functional impairment, leading to a failure in supporting neuron homeostasis.[39]

All these findings support that GFAP can be a helpful biomarker for disease follow-up until the very late phases. Most importantly, serum GFAP levels were associated with AD neuropathological stages and increased along with the severity of AD-related pathology.

Another relevant finding of our study was the independent association of serum GFAP levels with other neuropathological lesions, like AGD and HS. Although the degree of co-pathology in our cohort was very high, we found that AD pathology (ADNC) did not mediate these associations. The two previous studies assessing co-pathologies did not find associations with plasma GFAP. Winder *et al.*[18] only studied cerebral amyloid angiopathy, arteriolosclerosis or chronic vascular disease. Salvadó and colleagues[19] found that GFAP plasma levels did not predict the following co-pathologies: CAA, TDP43, LBD or AGD. They did not assess HS directly, but TDP43. Another factor is the differences in the time from blood extraction to the brain study, which is significantly shorter (139 days) in our study compared to 1.53 years (Bermudez *et al.*[20]), more than 2 years (Winder *et al.*[18]) or 482 days (Salvadó *et al.*[19]).

HS is characterized by intense gliosis (subiculum and hippocampal cortex) accompanied by temporal lobe atrophy and frequently TDP43 pathology. Both changes have recently been subsumed within LATE. This entity commonly affects elderly individuals with AD, increasing the degree of atrophy and correlating with cognitive deterioration.[30] In our series, HS was very prevalent, mainly as a co-pathology, involving 69.7% of patients at an anterior level (including early HS stages described recently by our group). Classic (advanced) HS was observed in 45.2% and 36.4% of patients at an anterior and posterior hippocampal level, respectively. Interestingly, GFAP serum levels correlated with our suggested classification scheme, including early HS stages.

As for AGD, our results indicate a lower prevalence of this tauopathy in our series (12%) than expected in this age group and in association with AD. The high frequency of extremely advanced AD in our series (41.2% Braak stage VI and 62.8% Thal stage 5 patients) and the high degree of middle temporal lobe atrophy (52.4% of brains with severe atrophy) suggest that a substantial number of AGD cases may have been missed due to overlap of a high burden of tau-positive AD pathology or to extreme neuronal loss (and associated tau-positive grains) due to advanced AGD.[31,40] This could explain

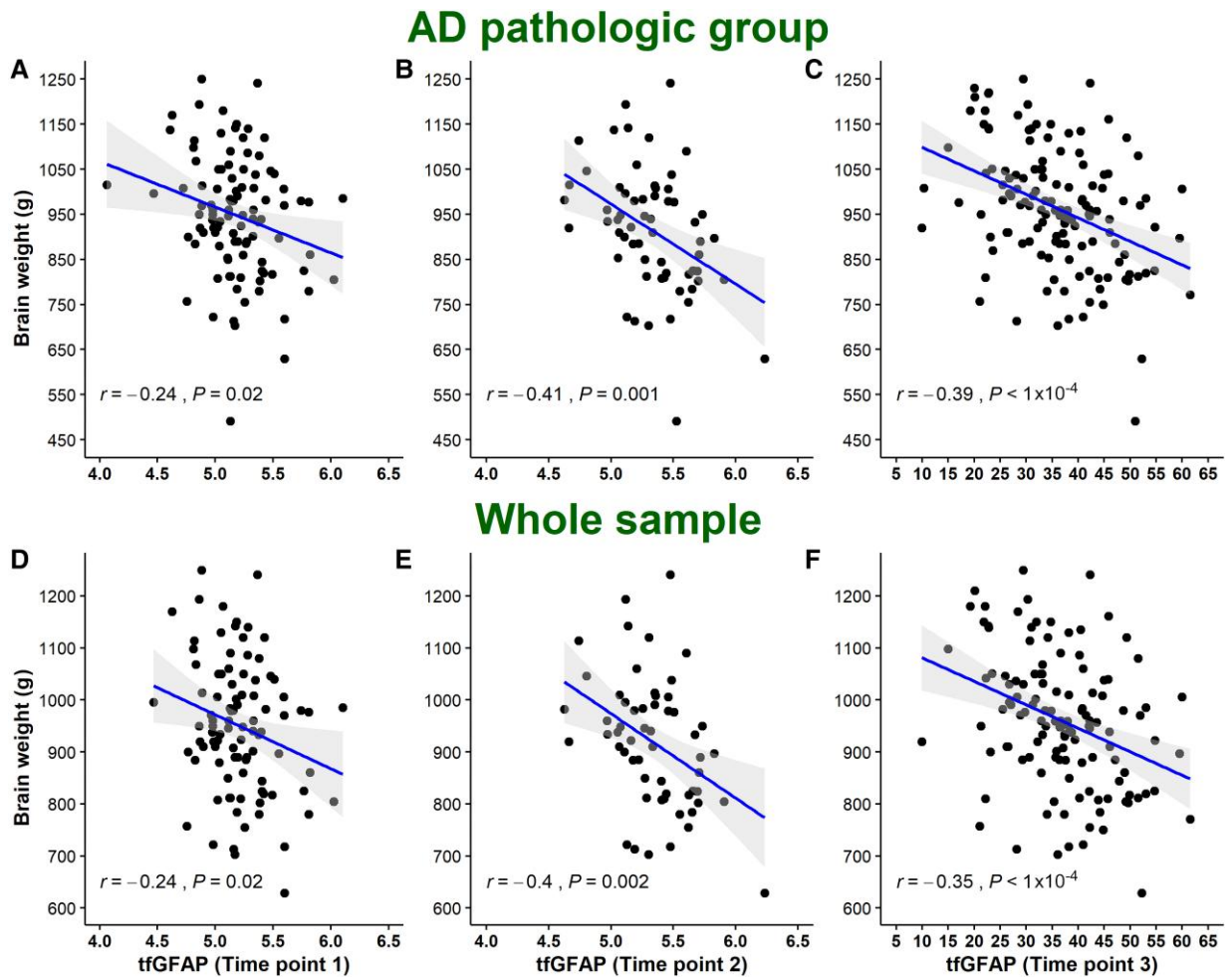

Figure 3 Correlation between tfGFAP and brain atrophy. AD = Alzheimer's disease; tfGFAP = GFAP levels normalized by the BoxCox transformation function.

the observed negative correlation between serum GFAP and AGD staging. If our findings are replicated in further studies, clinicians should bear in mind that blood GFAP levels might also partially be explained by these two pathologies specifically targeting the temporal lobes.

In addition to supporting the role of GFAP as an AD biomarker, our results provide insight into the relationship between astrocyte reactivity and AD pathology. GFAP is a crucial protein constituent of intermediate filaments, upregulated in reactive astrocytes.[41] In the context of AD, this process is thought to be initially triggered by amyloid deposition, which has been implicated in amyloid and tau clearing and in regulating inflammation and oxidative stress in the brain. However, astrocyte reactivity can become dysfunctional as the disease progresses, contributing to neuronal damage and cognitive decline.[42] Understanding this complex relationship is critical and could lead to new therapeutic approaches. A recent study has highlighted a relevant role for astrocyte reactivity in the AD continuum; in a large multicohort analysis, amyloid-β positivity was only associated with increased plasma phosphorylated tau in those individuals with positive astrocyte reactivity determined by plasma GFAP.[43]

Our study shows that pre-mortem GFAP levels are strongly correlated with AD pathology estimated by the NIA-A, NIA-B and NIA-C rating scales, further supporting that the astrocyte reactivity runs parallel to the AD neurodegenerative process. However, when we entered into the same explanatory model all ADNC components plus covariates, the only variable independently associated with GFAP levels was NIA-B. Therefore, in line with Salvadó *et al.*,[19] we found that the GFAP levels were associated mainly with the neurofibrillary tangles load. To further clarify this finding, we performed a mediation analysis to assess the relationships between the phenomena linked to GFAP levels, amyloid plaques (NIA-A and NIA-C) and tau tangles neuropathological load (NIA-B). We found a main pathway directly linking both amyloid variables, NIA-A and NIA-C, to tau (NIA-B). There was also evidence of an independent alternative pathway that, starting from amyloid, modified tau load via GFAP serum levels at time point 3, suggesting a mediator role of reactive astrocytes in AD-related tau pathology. This finding contrasts with previous cross-sectional studies using CSF or amyloid PET as the gold standard for AD pathology, in which GFAP was predominantly associated with amyloid.[11] The only study that has analysed the association with amyloid and tau jointly using PET reported that GFAP was only independently linked with amyloid pathology.[13]

Animal experimentation and human neuropathological studies show that astrocyte reactivity colocalizes with amyloid plaques and suggest that, together with the microglia, they could play a role in plaque phagocytosis.[42,44-46] Their relationship with

Table 3 Association between levels of serum tfGFAP and post-mortem neuropathology

Model	Independent variables	β (95% CI)	P-value	R^2	AIC_c
Basic model[a]	Covariates	–	–	0.13	1011.147
NIA-A[b]	Intermediate	−10.27 (−21.72, 1.19)	0.079	0.21	1000.603
	High	3.19 (−6.12, 12.49)	0.499		
NIA-B[c]	Intermediate	**7.17 (0.13, 14.21)**	0.046	**0.25**	**985.558**
	High	**12.85 (7.11, 18.6)**	<0.001		
NIA-C[d]	Intermediate	0.74 (−4.95, 6.44)	0.796	0.16	1009.279
	High	**4.69 (0.31, 9.07)**	0.036		
NIA-A+	Intermediate NIA-A	−6.67 (−19.25, 5.91)	0.296	**0.26**	**989.117**
NIA-B+	High NIA-A	−0.98 (−14.89, 12.92)	0.889		
NIA-C[e]	Intermediate NIA-B	7.00 (−3.5, 17.51)	0.190		
	High NIA-B	**13.23 (2.06, 24.39)**	0.021		
	Intermediate NIA-C	−5.28 (−11.71, 1.16)	0.107		
	High NIA-C	−3.05 (−9.39, 3.29)	0.344		
ADNC[f]	Intermediate	**8.48 (1.69, 15.28)**	0.015	0.20	1002.574
	High	**10.35 (4.63, 16.06)**	<0.001		

The reference group in each case, for NIA-A, NIA-B and NIA-C groups, was their respective lower category (Non/Low NIA-A, Non/Low NIA-B, Non/Low NIA-C). Intermediate Alzheimer's disease neuropathologic change (ADNC) comprises individuals with post-mortem neuropathology classified as 2 and high as 3. Covariates included in the models are age at serum extraction, estimated age at onset, number of days between last serum collection and death date, and sex. Significant coefficients and better goodness-of-fit indexes are in bold. AIC_C = corrected Akaike criterion; CI = confidence interval; NIA-(A–C) = National Institute on Aging ABC method of assessing ADNC; R^2 = adjusted R^2; tfGFAP = GFAP levels normalized by the BoxCox transformation function.

[a]Basic model equation: $tfGFAP_{T3} = b_0 + b_1 \times \text{Age extraction} + b_2 \times \text{Age onset} + b_3 \times \text{T3-exitus} + b_4 \times \text{Sex}$.

[b]Model equation: $tfGFAP_{T3} = b_0 + b_1 \times \text{NIA-A} + b_2 \times \text{Age extraction} + b_3 \times \text{Age onset} + b_4 \times \text{T3-exitus} + b_5 \times \text{Sex}$.

[c]Model equation: $tfGFAP_{T3} = b_0 + b_1 \times \text{NIA-B} + b_2 \times \text{Age extraction} + b_3 \times \text{Age onset} + b_4 \times \text{T3-exitus} + b_5 \times \text{Sex}$.

[d]Model equation: $tfGFAP_{T3} = b_0 + b_1 \times \text{NIA-C} + b_2 \times \text{Age extraction} + b_3 \times \text{Age onset} + b_4 \times \text{T3-exitus} + b_5 \times \text{Sex}$.

[e]Model equation: $tfGFAP_{T3} = b_0 + b_1 \times \text{NIA-A} + b_2 \times \text{NIA-B} + b_3 \times \text{NIA-C} + b_4 \times \text{Age extraction} + b_5 \times \text{Age onset} + b_6 \times \text{T3-exitus} + b_7 \times \text{Sex}$.

[f]Model equation: $tfGFAP_{T3} = b_0 + b_1 \times \text{ADNC} + b_2 \times \text{Age extraction} + b_3 \times \text{Age onset} + b_4 \times \text{T3-exitus} + b_5 \times \text{Sex}$.

neurofibrillary tangles is less studied; however, it has also been documented, although it is pointed out that it will occur only in later disease stages when reactive astrocytes interact with ghost tangles.[47,48] Therefore, GFAP levels may be influenced by both types of AD pathological signatures and other factors, such as inflammation or co-pathologies. Those influences might vary along the disease course. Therefore, a possible explanation reconciling the findings reported by Salvadó *et al.*,[19] replicated in our study, with previous results of cross-sectional studies could be related to the dynamic nature of the role played by astrocytes. In cross-sectional studies performed mainly in individuals with early-middle disease stages, amyloid pathology could be the main driver behind GFAP levels. However, in neuropathological studies where we can observe the last disease stages, we might be able to detect the interactions with tau pathology better. Supporting this view, a quantitative stereology-based post-mortem study has reported that glial responses (astrocytes and microglia) increase linearly around existing plaques and near tangles; however, while astrocytes correlated with tau burden, they did not find a correlation with the amyloid load.[49] Taken together, these results indicate that the progression of astrocyte reactivity, estimated by GFAP levels, might diverge from that of amyloid deposition at some point during the disease course explaining the different results in clinical cross-sectional and neuropathological studies.

To the best of our knowledge, our results provide, for the first time, direct evidence in humans that antemortem serum GFAP reflects astrocyte reactivity estimated by the GFAP-immunostained brain areas. The observed trend towards higher correlations in individuals with an increased tau load aligns with our concurrent observation of an association between serum GFAP and neurofibrillary tangle pathology. Also, in congruence with our previous results, we found that the GFAP-immunostained area in the entorhinal cortex negatively correlated with brain weight.

Our quantitative pathology analysis revealed spatially dependent weak correlations between serum GFAP and the GFAP-immunostained brain area. This pattern should be interpreted within the intricate context of astrocyte involvement in AD, wherein diverse phenotypes manifest at distinct disease stages in a sort of 'astrocytic continuum', ranging from astrocyte reactivity with hypertrophy to atrophy with loss of function.[39] In parallel with these observations, studies determining plasma GFAP levels and PET imaging with the astrocyte tracer ^{11}C-deuterium-L-deprenyl in familial AD individuals have depicted divergent trajectories, suggesting that both astrocyte biomarkers might reflect different states or subtypes of astrocyte reactivity.[50] Given the spatial progression characteristic of AD, it is plausible that diverse regions may exhibit varying disease activity and, consequently, diverse, overlapping astrocyte phenotypes. Thus, in neuropathological studies, variations are expected depending on the sampled brain region.

Our data support the hypothesis that serum GFAP levels may serve as an indicator of overall astrocyte reactivity, encapsulating the cumulative effects of regions with heightened disease activity. However, to understand these intricate relationships, studies incorporating a more comprehensive sampling of diverse brain regions at various disease stages are warranted.

Additionally, we aimed to investigate the relationship between serum GFAP and microglial activation, given the significant cross-talk between astrocytes and microglia. In a subsample of advanced AD patients (Braak > 4), we used the CD68 area as a proxy for microglial activation. We observed a negative correlation between the immunostained area of CD68 in the entorhinal cortex and serum GFAP. In the context of AD, both microglia and astrocyte activation have been reported to manifest with a spatial and temporal distinct pattern, with microglia activation occurring before astrocyte activation.[51] It is important to note that our findings are limited to a specific group of advanced AD patients and to a single region of the brain (the entorhinal cortex). To gain a more complete

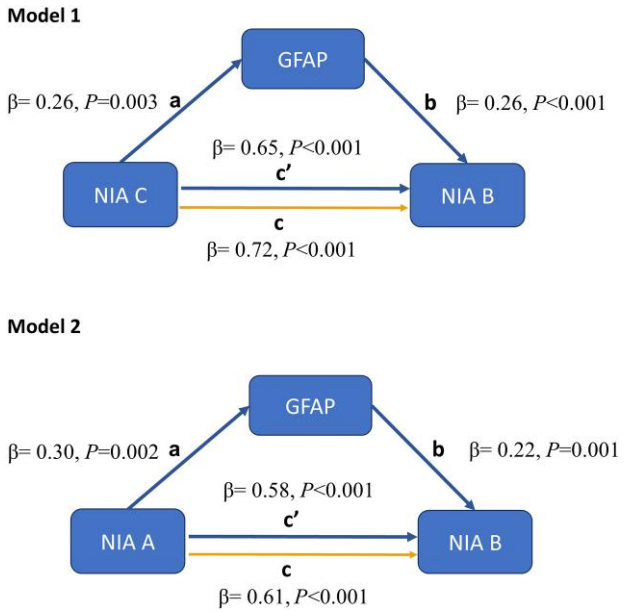

Figure 4 Parameters estimated trough partial mediation model with serum GFAP (time point 3) as mediator between amyloid (NIA-A and NIA-C) and tau loads (NIA-B). Both models get acceptable goodness-of-fit indexes, root mean square error of approximation (RMSEA) = 0.067, comparative fit index (CFI) = 0.98, Tucker–Lewis index (TLI) = 0.96 and standardized root mean residual (SRMR) = 0.052 (n = 138) at the first model, and for the second model, RMSEA = 0.057, CFI = 0.98, TLI = 0.97 and SRMR = 0.054 (n = 138). NIA-(A–C) = National Institute on Aging ABC method of assessing Alzheimer's disease neuropathologic change.

understanding of the relationship between serum GFAP and the status of microglia, we will need to conduct further research with larger sample sizes that cover various brain regions and disease stages.

The design of our study, following a cohort of dementia patients from a nursing home, has important advantages but also has some limitations. One potential issue is the predominance of AD dementia and the female gender. These are both intrinsic characteristics of our cohort, which is representative of institutionalized old dementia individuals, but it might limit the generalization of our results to different settings. Another potential limitation is the lack of major neurovascular pathology in our series, which might have influenced our inability to find an association between GFAP levels and vascular pathology, as others have previously reported.[52] The fact that our sample is composed of late-stage dementia individuals limits the generalizability of our results regarding diagnostic accuracy in earlier disease stages or the potential utility of GFAP as a screening tool for AD.

A particularity of our study is that we measured GFAP in serum instead of plasma, unlike previous reports that linked blood GFAP levels with neuropathology.[18-20] We used a Quanterix kit, which is designed and validated for both plasma and serum measurement (Simoa® Neurology 2-Plex B Kit; SR-X® Data Sheet). Consequently, our data provide further validation and confirmation of previous findings by replicating the results observed in plasma using serum samples. Among the main strengths, the close follow-up of the patients allows for the extremely short time elapsed from the serum extraction to the autopsy, which increases temporal precision and minimizes bias. Additionally, our study is the first to correlate longitudinal GFAP data with neuropathology, increasing the robustness of the analysis.

Our findings have several implications for clinicians. We show evidence that: (i) serum GFAP correlates with AD neuropathology; (ii) serum GFAP is a good biomarker for AD in patients with advanced dementia; (iii) serum GFAP levels increase progressively with the disease course and correlate with cognitive deterioration; (iv) individuals with younger age at onset tend to have higher levels of serum GFAP; and (v) some AD co-pathologies like HS or AGD might influence serum GFAP levels.

In conclusion, our results contribute to the growing body of evidence suggesting the role of blood GFAP as a diagnostic biomarker and offer mechanistic insights into its relationship with AD neuropathology, highlighting its ties with tau burden. Additionally, our analysis revealed an independent association between serum GFAP levels and other neuropathological lesions, such as AGD and HS, suggesting the involvement of reactive astrocytes in these pathologies. The longitudinal design and correlation with post-mortem data reinforce the robustness of our findings. However, data correlating blood biomarkers and neuropathological assessments are still scant, and further research is needed to replicate and validate these results in diverse populations.

Data availability

The VACS cohort is an ongoing study. Anonymized data can be accessed upon request at direccioncientifica@fundacioncien.es.

Acknowledgements

The authors wish to thank the participants of the Vallecas Alzheimer's Center Study (VACS) cohort and their family members. We also want to acknowledge the personnel at the Reina Sofía Center. This work has been supported by the Queen Sofia Foundation. PSJ is supported by grants from ISCIII (PMP22/00022 and PI20/01011) and TED2021-131676B-100.

Funding

This work has been supported by the Fundación Reina Sofia and Next Generation funding UE/Mecanismo de Recuperación y Resiliencia through projects PMP22/00022 (ISCIII) and TED2021-131676B-100. MCIN/AEI/10.13039/501100011033

Competing interests

The authors report no competing interests.

Supplementary material

Supplementary material is available at *Brain* online.

References

1. Zetterberg H, Blennow K. Moving fluid biomarkers for Alzheimer's disease from research tools to routine clinical diagnostics. *Mol Neurodegener*. 2021;16:10.
2. Teunissen CE, Verberk IMW, Thijssen EH, et al. Blood-based biomarkers for Alzheimer's disease: Towards clinical implementation. *Lancet Neurol*. 2022;21:66-77.
3. Fukuyama R, Izumoto T, Fushiki S. The cerebrospinal fluid level of glial fibrillary acidic protein is increased in cerebrospinal fluid

from Alzheimer's disease patients and correlates with severity of dementia. *Eur Neurol*. 2001;46:35-38.
4. Jesse S, Steinacker P, Cepek L, et al. Glial fibrillary acidic protein and protein S-100B: Different concentration pattern of glial proteins in cerebrospinal fluid of patients with Alzheimer's disease and Creutzfeldt-Jakob disease. *J Alzheimers Dis*. 2009;17:541-551.
5. Ishiki A, Kamada M, Kawamura Y, et al. Glial fibrillar acidic protein in the cerebrospinal fluid of Alzheimer's disease, dementia with Lewy bodies, and frontotemporal lobar degeneration. *J Neurochem*. 2016;136:258-261.
6. Abu-Rumeileh S, Steinacker P, Polischi B, et al. CSF biomarkers of neuroinflammation in distinct forms and subtypes of neurodegenerative dementia. *Alzheimers Res Ther*. 2019;12:2.
7. Oeckl P, Halbgebauer S, Anderl-Straub S, et al. Glial fibrillary acidic protein in Serum is increased in Alzheimer's disease and correlates with cognitive impairment. *J Alzheimers Dis*. 2019;67:481-488.
8. Zhu N, Santos-Santos M, Illán-Gala I, et al. Plasma glial fibrillary acidic protein and neurofilament light chain for the diagnostic and prognostic evaluation of frontotemporal dementia. *Transl Neurodegener*. 2021;10:50.
9. Simrén J, Weninger H, Brum WS, et al. Differences between blood and cerebrospinal fluid glial fibrillary acidic protein levels: The effect of sample stability. *Alzheimers Dement*. 2022;18:1988-1992.
10. Verberk IMW, Thijssen E, Koelewijn J, et al. Combination of plasma amyloid beta(1–42/1–40) and glial fibrillary acidic protein strongly associates with cerebral amyloid pathology. *Alzheimers Res Ther*. 2020;12:118.
11. Chatterjee P, Pedrini S, Stoops E, et al. Plasma glial fibrillary acidic protein is elevated in cognitively normal older adults at risk of Alzheimer's disease. *Transl Psychiatry*. 2021;11:27.
12. Benedet AL, Milà-Alomà M, Vrillon A, et al. Differences between plasma and cerebrospinal fluid glial fibrillary acidic protein levels across the Alzheimer disease Continuum. *JAMA Neurol*. 2021;78:1471.
13. Pereira JB, Janelidze S, Smith R, et al. Plasma GFAP is an early marker of amyloid-β but not tau pathology in Alzheimer's disease. *Brain*. 2021;144:3505-3516.
14. Verberk IMW, Laarhuis MB, van den Bosch KA, et al. Serum markers glial fibrillary acidic protein and neurofilament light for prognosis and monitoring in cognitively normal older people: a prospective memory clinic-based cohort study. *Lancet Healthy Longev*. 2021;2:e87-e95.
15. Rajan KB, Aggarwal NT, McAninch EA, et al. Remote blood biomarkers of longitudinal cognitive outcomes in a population study. *Ann Neurol*. 2020;88:1065-1076.
16. Cicognola C, Janelidze S, Hertze J, et al. Plasma glial fibrillary acidic protein detects Alzheimer pathology and predicts future conversion to Alzheimer dementia in patients with mild cognitive impairment. *Alzheimers Res Ther*. 2021;13:68.
17. Bellaver B, Ferrari-Souza JP, Uglione da Ros L, et al. Astrocyte biomarkers in Alzheimer disease: A systematic review and meta-analysis. *Neurology*. 2021;96:e2944-e2955.
18. Winder Z, Sudduth TL, Anderson S, et al. Examining the association between blood-based biomarkers and human post mortem neuropathology in the University of Kentucky Alzheimer's Disease Research Center autopsy cohort. *Alzheimers Dement*. 2023;19:67-78.
19. Salvadó G, Ossenkoppele R, Ashton NJ, et al. Specific associations between plasma biomarkers and postmortem amyloid plaque and tau tangle loads. *EMBO Mol Med*. 2023;15:e17123.
20. Bermudez C, Graff-Radford J, Syrjanen JA, et al. Plasma biomarkers for prediction of Alzheimer's disease neuropathologic change. *Acta Neuropathol (Berl)*. 2023;143:487-503.
21. Therriault J, Vermeiren M, Servaes S, et al. Association of phosphorylated tau biomarkers with amyloid positron emission tomography vs tau positron emission tomography. *JAMA Neurol*. 2023;80:188-199.
22. Martínez-Martín P, Avila J, AD Research Unit Investigators. Alzheimer Center Reina Sofia Foundation: Fighting the disease and providing overall solutions. *J Alzheimers Dis*. 2010;21:337-348.
23. Harrell LE, Marson D, Chatterjee A, Parrish JA. The severe Mini-Mental State Examination: a new neuropsychologic instrument for the bedside assessment of severely impaired patients with Alzheimer disease. *Alzheimer Dis Assoc Disord*. 2000;14:168-175.
24. Ortega-Cruz D, Uceda-Heras A, Iglesias JE, Zea-Sevilla MA, Strange B, Rabano A. A novel histological staging of hippocampal sclerosis that is evident in gray matter loss in vivo. *Alzheimers Dement*. 2023;19:3028-3040.
25. Montine TJ, Phelps CH, Beach TG, et al. National Institute on Aging-Alzheimer's association guidelines for the neuropathologic assessment of Alzheimer's disease: A practical approach. *Acta Neuropathol (Berl)*. 2012;123:1-11.
26. Braak H, Del Tredici K, Rüb U, de Vos RAI, Jansen Steur ENH, Braak E. Staging of brain pathology related to sporadic Parkinson's disease. *Neurobiol Aging*. 2003;24:197-211.
27. Attems J, Toledo JB, Walker L, et al. Neuropathological consensus criteria for the evaluation of Lewy pathology in post-mortem brains: A multi-centre study. *Acta Neuropathol (Berl)*. 2021;141:159-172.
28. Deramecourt V, Slade JY, Oakley AE, et al. Staging and natural history of cerebrovascular pathology in dementia. *Neurology*. 2012;78:1043-1050.
29. Skrobot OA, Attems J, Esiri M, et al. Vascular cognitive impairment neuropathology guidelines (VCING): The contribution of cerebrovascular pathology to cognitive impairment. *Brain*. 2016;139:2957-2969.
30. Nelson PT, Dickson DW, Trojanowski JQ, et al. Limbic-predominant age-related TDP-43 encephalopathy (LATE): Consensus working group report. *Brain*. 2019;142:1503-1527.
31. Saito Y, Ruberu NN, Sawabe M, et al. Staging of argyrophilic grains: An age-associated tauopathy. *J Neuropathol Exp Neurol*. 2004;63:911-918.
32. Kovacs GG, Ferrer I, Grinberg LT, et al. Aging-related tau astrogliopathy (ARTAG): Harmonized evaluation strategy. *Acta Neuropathol (Berl)*. 2016;131:87-102.
33. Carpenter AE, Jones TR, Lamprecht MR, et al. CellProfiler: Image analysis software for identifying and quantifying cell phenotypes. *Genome Biol*. 2006;7:R100.
34. Nichols E, Merrick R, Hay SI, et al. The prevalence, correlation, and co-occurrence of neuropathology in old age: Harmonisation of 12 measures across six community-based autopsy studies of dementia. *Lancet Healthy Longev*. 2023;4:e115-e125.
35. Beauducel A, Herzberg PY. On the performance of Maximum likelihood versus means and variance adjusted weighted least squares estimation in CFA. *Struct Equ Model*. 2006;13:186-203.
36. Hu L, Bentler PM. Cutoff criteria for fit indexes in covariance structure analysis: Conventional criteria versus new alternatives. *Struct Equ Model*. 1999;6:1-55.
37. Sutphen CL, McCue L, Herries EM, et al. Longitudinal decreases in multiple cerebrospinal fluid biomarkers of neuronal injury in symptomatic late onset Alzheimer's disease. *Alzheimers Dement*. 2018;14:869-879.

38. Therriault J, Pascoal TA, Lussier FZ, et al. Biomarker modeling of Alzheimer's disease using PET-based Braak staging. *Nat Aging*. 2022;2:526-535.
39. Verkhratsky A, Rodrigues JJ, Pivoriunas A, Zorec R, Semyanov A. Astroglial atrophy in Alzheimer's disease. *Pflugers Arch*. 2019; 471:1247-1261.
40. Rábano A, Rodal I, Cuadros R, Calero M, Hernández F, Ávila J. Argyrophilic grain pathology as a natural model of tau propagation. *J Alzheimers Dis*. 2014;40(Suppl 1):S123-S133.
41. Escartin C, Galea E, Lakatos A, et al. Reactive astrocyte nomenclature, definitions, and future directions. *Nat Neurosci*. 2021;24: 312-325.
42. Perez-Nievas BG, Serrano-Pozo A. Deciphering the astrocyte reaction in Alzheimer's disease. *Front Aging Neurosci*. 2018;10:114.
43. Bellaver B, Povala G, Ferreira PCL, et al. Astrocyte reactivity influences amyloid-β effects on tau pathology in preclinical Alzheimer's disease. *Nat Med*. 2023;29:1775-1781.
44. Itagaki S, McGeer PL, Akiyama H, Zhu S, Selkoe D. Relationship of microglia and astrocytes to amyloid deposits of Alzheimer disease. *J Neuroimmunol*. 1989;24:173-182.
45. Frost GR, Li YM. The role of astrocytes in amyloid production and Alzheimer's disease. *Open Biol*. 2017;7:170228.
46. Beach TG, McGeer EG. Lamina-specific arrangement of astrocytic gliosis and senile plaques in Alzheimer's disease visual cortex. *Brain Res*. 1988;463:357-361.
47. Ikeda K, Haga C, Akiyama H, Kase K, Iritani S. Coexistence of paired helical filaments and glial filaments in astrocytic processes within ghost tangles. *Neurosci Lett*. 1992;148(1–2): 126-128.
48. Ikeda K, Haga C, Oyanagi S, Iritani S, Kosaka K. Ultrastructural and immunohistochemical study of degenerate neurite-bearing ghost tangles. *J Neurol*. 1992;239:191-194.
49. Serrano-Pozo A, Mielke ML, Gómez-Isla T, et al. Reactive glia not only associates with plaques but also parallels tangles in Alzheimer's disease. *Am J Pathol*. 2011;179:1373-1384.
50. Chiotis K, Johansson C, Rodriguez-Vieitez E, et al. Tracking reactive astrogliosis in autosomal dominant and sporadic Alzheimer's disease with multi-modal PET and plasma GFAP. *Mol Neurodegener*. 2023;18:60.
51. Wu Y, Eisel ULM. Microglia-astrocyte communication in Alzheimer's disease. *J Alzheimers Dis*. 2023;95:785-803.
52. Elahi FM, Casaletto KB, La Joie R, et al. Plasma biomarkers of astrocytic and neuronal dysfunction in early- and late-onset Alzheimer's disease. *Alzheimers Dement*. 2020;16:681-695.